View metadata, citation and similar papers at core.ac.uk
brought to you by CORE
provided by CiteSeerX

Proceedings of IMECE2002
ASME International Mechanical Engineering Congress & Exposition
November 17-22, 2002, New Orleans, Louisiana

IMECE2002-39584

ELECTRONICS SPOT COOLING WITH LIQUID NITROGEN

M. Rada, A. Shooshtari, M. Ohadi, F. H. R. França
S^2TS – Smart and Small Thermal Systems Laboratory
Department of Mechanical Engineering
University of Maryland, College Park, MD 20742

J. Lawler
Advanced Thermal and Environmental Concepts, Inc.
387 Technology Drive, Suite 2110, College Park, MD 20742

ABSTRACT
This paper describes an ongoing research to evaluate and characterize electrohydro-dynamic (EHD) meso- and micro-pumps for spot cooling of sensors. In the proposed concept, the localized cooling is achieved by means of a flow of liquid nitrogen that is driven by an ion-drag pump towards the heat source, where heat is directly removed. First, a numerical heat transfer model will illustrate the advantages of the proposed concept of spot cooling with liquid nitrogen against a conventional conduction cooling. Next, we will present experimental results for pumping of liquid nitrogen via (EHD) a pump at the meso-scale, as well as experiments with EHD micro-pumps for pumping of HFE-7100 at room temperature. The objective of this research is to establish the optimum operational and design conditions for micro-pumping of liquid nitrogen for spot cooling applications.

1. INTRODUCTION
Electronics Cooling can strongly benefit from a source integrated micro-cooling device, which incorporates active microscale heat, transfer surfaces, micropumps, and temperature and pressure sensors in one single package directly attached to the heat source. The objective of this research is to develop meso- and micro-pumps capable of establishing the necessary pumping head to generate a flow capable of providing the required heat transfer from electronic components. The meso- and micro-pumps are based on the electro-hydrodynamic (EHD) ion-drag induced flow.

The research involves two distinct but complementary experimental investigations. The first one is being carried out in the cryogenic facilities at NASA Goddard Space Flight Center, and tackles EHD pumping of liquid nitrogen. The second investigation is being performed in the S^2TS laboratory at the University of Maryland, College Park, to study the pumping capabilities of EHD micro-pumps. The experiments are being carried out with HFE-7100 cooling liquid at room temperature. In parallel to these experiments, an additional effort is underway to tackle the numerical solution of the EHD pumping of liquids in complex 3D geometries. This is a valuable tool for optimization of the performance of EHD injection pumps.

This work is organized as follows. First, the concept of spot cooling with liquid nitrogen is compared with conduction cooling since the proposed concept of spot cooling requires that liquid nitrogen to be directly taken to the heat source device by an EHD ion-drag pump. The next section describes experimental and theoretical investigations of a meso-pump for pumping liquid nitrogen at cryogenic conditions, and different designs of micro-pump for pumping HFE-7100 at room temperatures. The thermal properties of these two fluids, at the respective test temperatures, are presented in Table 1.

2. MOTIVATION OF THE PROPOSED CONCEPT
The concept of source-integrated cooling of sensors at cryogenic temperatures is illustrated in Fig. 1. Instead of cooling the entire board where the sensors are located, this concept allows the cooling to occur right on the heat source. Heat is extracted from the sensors by liquid nitrogen that flows in a channel directly attached to the sensors. As proposed in this work, the force to drive the liquid nitrogen through the channel and connecting line is provided by an EHD ion-drag pump that is part of the channel itself. Such pumps are discussed in Section 3 of this paper. After liquid nitrogen absorbs heat from the sensors, it is then circulated in a loop towards a cryocooler where it is cooled. In this process, only sensible heat is involved with no phase change. Additional ion-drag pumps can be installed in the loop duct lines to compensate for additional pressure losses.

In order to demonstrate the advantages of a cryogenic loop for cooling high-powered sensors, a numerical simulation of the process was carried out for comparison with a conduction cooling system. Figure 2 shows two propositions for cooling of an electronic device. In case (a), liquid nitrogen flows in a channel that is directly attached to the chip board. The liquid nitrogen enters at a cryogenic temperature T_c after it undergoes cooling in a cryocooler. In case (b), the chip board is attached to a copper strap that is in direct thermal contact with the

Copyright © 2002 by ASME

Downloaded From: https://proceedings.asmedigitalcollection.asme.org on 07/02/2019 Terms of Use: http://www.asme.org/about-asme/terms-of-use

cryocooler at T_c. It was assumed that the contact resistances in both cases were the same and thus, they were not considered in both numerical models. For the numerical solution, the following conditions were assumed. The chip, having length and width of 15 and 10 mm, has a power input of 0.5 W. The board is a silicon plate with length, width and thickness of 45, 30, and 2.0 mm, respectively, and has a thermal conductivity of 150 W/mK. In the first case, liquid enters the channel with a temperature of $T_c = 73$ K, and a mass flow rate of 1.0 g/s. The ion-drag pump is built in the channel that has a length of 18 mm, a width of 15 mm, and a height 0.15 mm. In case (b), the copper strap has a cross sectional area of 100 mm^2, and a length of 150 mm; its thermal conductivity is 400 W/mK.

Figure 3 compares the temperature distribution in the chip for spot cooling with liquid nitrogen and for conduction cooling. As seen, the numerical simulation demonstrates that spot cooling is capable of keeping the chip at cryogenic temperatures. In fact, for the selected conditions of this problem, it allows a lower temperature in the chip than it is obtained with conduction cooling through the copper strap. In addition, a few other advantages of spot cooling with liquid nitrogen can be pointed out. From a single cryocooler, several flow channels can be drawn to refrigerate electronic devices in different locations, which would be more difficult with conduction straps. Another advantage is that liquid nitrogen flowing in channel can be more easily insulate thermally from the environment than relatively large conduction elements.

The next section describes two parallel efforts to drive liquid nitrogen with an ion-drag meso-pump and to pump a room temperature cooling fluid (HFE-7100) with a micro-pump. The goal is prove the capabilities of pumping liquid nitrogen with an EHD ion-drag pump, and in the next stage, use micro-pumps to pump liquid nitrogen in a cooling loop, as required in the proposed source-integrated concept.

3. ION-DRAG EHD PUMPS

3.1. Background

When a high electric field is set between properly designed electrodes, ions can be generated in the region of highest electric field. Once the ions are formed, they move towards the electrode with opposite polarity, dragging neutral molecules and causing movement of the bulk flow of the fluid. This is the basic principle of ion-drag pumps. Though this mechanism has been known for about a century, only in recent decade it has raised considerable interest for real applications. Its advantages include lack of moving parts, controllability, and its requirement of very small power consumption in the order of milliwatts or lower. Ion-drag pumping is a promising technology for electronic cooling because one of its strictest requirements – a clean environment – is usually an already existing condition. Besides, it can be used for pumping of cryogenic dielectric liquids, which are becoming a widely adopted technique for cooling of high-power electronic devices in conventional and space systems. The long-term effect of electric field on the liquid molecular structure has not been fully understood and reported. However, since cryogenic liquids exhibit relatively simple and stable molecular structures, they are expected to show a better repeatability of the results. For this reason, this ongoing project aims at the design, development and test of ion-drag pumps for cryogenic liquids.

When an electric field is applied to a dielectric fluid, secondary motions are induced within the fluid in the presence of charges. The pumping effect is achieved when the charged species move in the direction of the electrode with opposite polarity, colliding with the neutral molecules along the way, and setting a motion in the fluid. This type of EHD pump is designated as ion-drag pump. The general relation for electric field force acting on the fluid molecules is given by:

$$\vec{F}_e = \rho_c \vec{E} - \frac{\varepsilon_0}{2} E^2 \nabla k + \frac{\varepsilon_0}{2} \nabla\left(E^2 \rho_m \frac{dk}{d\rho_m} \right) \qquad (1)$$

where ρ_c and ρ_m are the charge and mass density of the fluid, E is the electric field intensity, ε_0 is the dielectric permitivity of vacuum, and k is the dielectric constant of the fluid. The first term in Eq. (1) represents the Coulomb force, also called the electrophoretic force, acting on the charged species within the fluid. The charged species in a dielectric fluid can be obtained through ionization in the vicinity of one electrode. The body force will drag these species towards the electrode with opposite polarity. This component of the EHD body force is the most important contribution to ion-drag pumping. The second component of Eq. (1) is the dielectrophoretic force, which is related to the gradients of the dielectric constant in the fluid medium. The third term in Eq. (1) is the electrostrictive force, and is related to the electric field non-homogeneity within the dielectric medium. In a single-phase fluid, the last two terms of Eq. (1) can be neglected, so the pumping force in the fluid is solely related to the Coulomb force:

$$\vec{F}_e = \rho_c \vec{E} \qquad (2)$$

As discussed, pumping in a single-phase fluid is possible only if charge is first generated in the fluid. Ion injection occurs through ion generation at the metal-liquid interface. This is achieved with the use of electrodes with sharp points or edges, where the small radius of curvature intensifies the electric field to a point where ionization of the dielectric fluid takes place. These electrodes are denominated emitters. The electrodes that attract the formed ions and absorb their charges are known as the collectors.

Several types of electrode designs have been proposed in the literature: a grid type emitter and collector, a drilled-holes plate electrode, ring electrodes, a needle type, and a screen with needles. Electrode designs for ion-drag pumping have been proposed in Stuetzer [1959], Sharbaugh and Walker [1985], Barbini and Coletti [1995], Bryan and Yagoobi [1990, 1990, 1992, 1994], Castaneda and Yagoobi [1991], and Rada et al. [2001]. A comprehensive study of electrode designs and materials for EHD applications can be found in Rada et al. [2001]. The basic design idea is to have one electrode with a small radius of curvature so that an intense electric field is generated for ionization of the liquid. The process occurs in a small region in the vicinity of the emitter, from where the formed ions are injected into the bulk flow and move towards the collector. It matters that the collector has less sharp edges than the emitter to avoid injections of ions of opposite polarity in the fluid. The presence of both negative and positive charges would result in a null net force in the fluid, with no pumping effect.

Copyright © 2002 by ASME

Downloaded From: https://proceedings.asmedigitalcollection.asme.org on 07/02/2019 Terms of Use: http://www.asme.org/about-asme/terms-of-use

3.2. Ion-drag mesopump for pumping of liquid nitrogen

The proposed meso-pump design for pumping of liquid nitrogen is discussed in detail in Rada et al. [2001]. Based on preliminary theoretical studies and the data available in the literature, the design consisted of a ring emitter with integrated needles around its circumference. The emitter was made of a stainless steel 316. A stainless steel block was first machined to form a conical shape on the internal surface and a cylindrical and conical shape on the external surface. Then, electrical discharge machining (EDM) machine was used to cut thirty teeth with a distance of 1.5 mm from the tip to the base plane. The geometry was designed to minimize the pressure drop effect in the pump itself, and to inject ions as close to the wall as possible (where the shear stress and temperature gradients are the highest). The collector was also made of a 316 stainless steel ring and placed coaxially with the emitter in the flow path. The distance between the tips of the emitter and collector was 2.5 mm. Also, the distance between the base of the emitter needles and the collector was 4.0 mm. The schematic of the meso-pump is presented in Fig. 4.

Another design requirement was that the electrical and pressure fittings must be compatible with cryogenic temperatures and pressures. Three Teflon PTFE cylindrical parts were mounted together to ensure the electrical isolation between the emitter and collector and between the electrodes and pump casing. The Teflon parts were made of a cylindrical rod that was bored through to give a 9.5 mm (3/8 in) inner diameter. They were then machined to allow electrical connections to the electrodes. The electrodes were connected to the power supply via two electrode feedthroughs that were well suited for the pressure and voltage ranges of interest. The loop was designed to conduct single-phase liquid nitrogen tests. The loop can withstand charging pressures on the order of 26 bars, and maintain a liquid phase inside the loop during pumping. The loop consists of the following components: the EHD meso-pump, an electrical (resistive) heater attached to a substrate with sufficient thermal mass that will provide the thermal load, a cryocooler connected through an interface to the cold side of the heat exchanger to maintain a liquid phase in the system, a liquid line, G-10 supports to suspend the loop and the reservoir with a minimum conduction heat transfer, a two-phase accumulator to provide temperature and pressure stability and controllability, and a copper shroud to minimize radiation heat transfer. A diagram and other details of the loop can be found in Rada et al. [2001].

The main objective of the meso-pump experiments was evaluation of the generated pressure head or the mass flow rate of liquid nitrogen. Measuring the pressure head provided by the meso-pump proved to be a difficult task due to the need of an accurate pressure sensor compatible for cryogenic temperatures. For that reason, an alternative method was proposed to measure the mass flow rate of liquid nitrogen based on a thermal energy balance in the loop. Figure 5 shows a schematic of the testing loop for the liquid nitrogen EHD meso-pump, showing the electrical heater attached to the liquid line, the cryocooler, the EHD meso-pump, and three silicon diodes for measurement of the temperatures on the wall of the liquid line, indicated by T_{w0}, T_{w1} and T_{w2}.

When the meso-pump is not operating, the heat that is provided by the electric heater (on the right in the loop schematic) is mainly conducted through the walls of the loop to the cryocooler. Preliminary calculations showed that the heat conducted through the liquid nitrogen line is negligibly small in comparison to the copper walls of the liquid line. In the same way, a detailed analysis of heat transfer through the supports of the loop, electric wiring, nitrogen liquid line and pressure measurement connections indicate that it is less than 5.0 % of the total heat input, and was also neglected. After the pump was turned on, liquid nitrogen flows through the line and absorbs part of the heat provided in the heater. The mass flow rate of the liquid nitrogen is computed by:

$$\dot{m}_{N2} = \frac{\dot{Q}_{N2}}{c_{p,N2}\Delta T_{N2}} \quad (3)$$

Although Eq. (3) is a straightforward result of the energy balance in the liquid nitrogen flow, it is a less obvious task to determine what is the fraction of the total heat that is absorbed by the liquid nitrogen, and the increase in the bulk temperature of the liquid nitrogen, ΔT_{N2}. This is considered next.

Since it is expected that the mass flow rate is small and the locations of the temperature measurements are reasonably away from bends in the line, it is assumed that the liquid nitrogen flow is fully developed. As a result, the difference in the bulk temperature of the liquid nitrogen in the control volume shown in Fig. 5 equals the difference in the measured temperatures of the wall. In other words, $\Delta T_{N2} = T_{w1} - T_{w2}$ where T_{w1} and T_{w2} are the measured temperatures on the line wall. The heat absorbed by the liquid nitrogen can be computed as the total heat input minus the heat conducted through the wall of the line; that is:

$$\dot{Q}_{N2} = \dot{Q}_{T} - \dot{Q}_{C} \quad (4)$$

The heat conducted through the copper walls are estimated in the following way. Figure 5 shows that the heat is conducted in the two branches of the line, 1 and 2, and are designated $\dot{Q}_{C1}$ and $\dot{Q}_{C2}$, which can be computed as:

$$\dot{Q}_{C1} = \frac{T_{w0} - T_{w1}}{R_1} \quad (5a)$$

$$\dot{Q}_{C2} = \frac{T_{w0} - T_{w2}}{R_2} \quad (5b)$$

where R_1 and R_2 are the thermal conduction resistances in section 0-1 and in section 0-2, respectively. Since the two branches are symmetrical between these two sections, the two resistances can be assumed the same, $R_1 = R_2 = R$. When there is not fluid flow in the loop (that is, when the EHD meso-pump is not operating), the heat conducted in branches 1 and 2 equals the total heat input, $\dot{Q}_T = \dot{Q}_{C1} + \dot{Q}_{C2}$. Using this relation together with Eqs. (5a) and (5) allows the estimation of the conduction resistance R. This was done for six different experiments (all of them without liquid nitrogen pumping), which are presented in Table 2. As seen, the conduction thermal resistance R presents values ranging from 2.06 to 2.95 K/W, with an average value of 2.41 K/W. This average value is taken for the computation of the heat absorbed by the liquid nitrogen when the pumps is under operation. The relation for the heat absorbed by the liquid nitrogen flow can be derived from Eqs. (4), (5a) and (5b):

$$\dot{Q}_{N2} = \dot{Q}_{T} - \frac{2T_{w0} - T_{w1} - T_{w2}}{R} \quad (6)$$

Copyright © 2002 by ASME

Downloaded From: https://proceedings.asmedigitalcollection.asme.org on 07/02/2019 Terms of Use: http://www.asme.org/about-asme/terms-of-use

Note that when the EHD meso-pump is operated, the measured temperature T_{w0}, T_{w1} and T_{w2} adjust to the presence of fluid flow convection. In the experiments, the meso-pump was first turned on to establish a fluid flow in the loop. After the system was stabilized, a total of 3.16 W was applied in the electric heater, and the temperatures on the walls were measured for the evaluation of the heat injected in the liquid nitrogen. The variation of the liquid nitrogen bulk temperature in the inlet and outlet of the control volume was also measured. The temperatures are shown in Table 3. As indicated, all temperatures were the same before heat was applied. (The temperatures were actually calibrated not to present any difference at the absence of heat input.) As heat is applied, the temperature in the exit of the control volume presents a higher value than that in the inlet, a condition expected when fluid flow is present. From the procedure described in this section, it was found that a flow rate of about 0.14 g/s of liquid nitrogen was achieved. This flow rate would be capable of absorbing a total heat of about 0.3 W for an elevation of 1 K in the temperature of liquid nitrogen, which is within the application for which this technology is devised.

3.3. Ion-drag micro-pump

In parallel to the experiments to drive liquid nitrogen with a meso-pump, an additional effort is focused on the development of ion-drag EHD micro-pumps. At this stage in the research, tests have been carried out to evaluate the performance of different micro-pump designs using HFE-7100 fluid at room temperatures (20 ^{o}C). Tests in such conditions are much simpler than those carried out in cryogenic temperatures, and so it allows an easy assessment of the performance of a number of different micro-pumps. In the next step, a set of optimum micro-pumps will be used for pumping liquid nitrogen in a cryogenic loop.

An example of micro-pump tested in this research is shown in Figs. 6(a) and 6(b). As seen, it consists basically of a rectangular alumina or silicon substrate where the electrodes are built in, and a top-case to close the channel and connect it to the manifolds of the cooling loop. Typical channel heights that have been fabricated and tested are 50, 100 and 200 µm. This flat geometry, similar to the one presented in the problem of Fig. 2, was especially designed to attach the micro-pump directly to the heating source. Two facilities in the University of Maryland at College Park were utilized for the microfabrication of the electrodes, the Mechanical Engineering Department and the Institute of Plasma Research. These facilities permit the assembling of micro-electrodes on the surface of alumina or silicon wafers using photolithography techniques. The electrodes are formed by metal layers (for example, niobium, gold or platinum), which are deposited on the substrate. The emitter usually presents a saw-tooth pattern to ensure ionization on the sharp tips, while the collectors are plain and smooth. This is shown in Fig. 7(a), in which the electrodes are separated by only 25 µm. In each micro-pump substrate, several pairs of emitter and collector electrodes are patterned, up to a total of 75 pairs of electrodes. Figure 7(b) shows three pairs of plain emitter and collector electrodes. As seen, electrodes of the same polarity are connected to each other to set the same voltage.

Different micro-pump designs have been tested in an open loop to determine the generated pressure head and electric current as a function of the applied voltage. Figure 8 shows such a result for micro-pumps having saw-tooth emitter and plain collectors separated by 20 and 50 µm so that the effect of the distance between the electrodes can be evaluated. As seen for both cases (20 and 50 µm), the electric current initially increases slowly with the voltage. For a dielectric liquid as the one tested in the experiment (HFE-7100), this small current is due to the presence of impurities. After a certain voltage, the current presents a sharp increase due to the onset of ionization. For the 20 µm micro-pump, the onset occurs at a voltage of about 300 V, while the onset is at about 400 V for the micro-pump with electrodes 50 µm apart. For a given voltage and electrode geometry, the shortest distance between the emitter and the collector gave the highest electric field strength. Considering that the onset electric field is the same in both cases and since the same dielectric fluid is used, then the ionization occurs at a lower voltage for electrodes with a smaller separation between the emitter and the collector.

The sharp increase in the pressure head coincides with the onset of ionization in the dielectric fluid. At this point, ions are formed and move towards the collectors, providing a force to create pressure head (no flow is present in this static test). Therefore, pumping starts at a lower voltage for the 20 µm micro-pump. Another advantage of having a smaller distance between the emitter and collector is that, for a given electric current, it requires a lower voltage, which means lower power consumption. For a pressure of 250 Pa, the power input is only 0.032 W.

An additional understanding of the phenomenon can be inferred from a numerical simulation of the electric field in the region between the emitter and the collector. The complete analysis of the EHD pumping mechanism require the solution of both the electric field and charge density distributions, which are given by a set of two coupled equations. They are given by:

$$\nabla^2\phi = -\frac{\rho_c}{\varepsilon} \qquad (7a)$$

$$\frac{\partial\rho_c}{\partial t} + \nabla\left[k\rho_c\nabla\phi\right] = 0 \qquad (7b)$$

The solution of the system of equations is further complicated by the absence of an obvious boundary condition for the charge density. One common approach is to use the electric current obtained from the experimental *i-V* curve as the input for the charge density, but this still requires a few assumptions regarding the ionization region in the emitter. Although this task is still under investigation, a simpler numerical simulation of the process can also be very useful for the micro-pump design. This is discussed next.

Considering the onset condition in which there is no charge present in the system, the potential field equation is given by the Laplace equation:

$$\nabla^2\phi = 0 \qquad (8)$$

This equation is then solved to find the electric field distribution in the micro-pump channel. Figure 9(a) shows the grid mesh for a computational module involving an emitter saw-tooth and a collector. Symmetry allows the extension of solution for this module to the remaining regions of the micro-pump channel. In this problem, in order to capture the smallest scales of electrode geometry and to achieve a grid independent solution, a total of 350,000 elements are used. This large

Copyright © 2002 by ASME

Downloaded From: https://proceedings.asmedigitalcollection.asme.org on 07/02/2019 Terms of Use: http://www.asme.org/about-asme/terms-of-use

number results from the resolution required in the sharp tip of the emitter electrode. Figure 9(b) presents the dimensionless electric field distribution in the computational domain. Based on the onset voltage of 400 V for this configuration (saw-tooth emitter separated by 50 μm from the plain collector), the electric field at the tip of the emitter is 200 V/μm after the dimensionless terms are properly converted to dimensional quantities. As reported in Gallagher [1975], most dielectric liquids present an onset electric field ranging from 130 to 480 V/μm, showing the adequacy of the numerical solution. In contrast, computing the onset electric field by the ratio between the applied voltage (400 V) over the distance between the electrodes (50 μm) would result in a value of only 8.0 V/μm.

4. CONCLUSIONS

This work discussed two parallel efforts that aim at the development of an EHD ion-drag micro-pump to drive liquid nitrogen. Such devices are an essential part of the concept of spot cooling of electronic devices, in which liquid nitrogen is taken directly to the chips for heat removal. A thermal hydraulic model of the process not only demonstrated the feasibility of this concept but also its capability of maintaining lower temperatures in the electronic devices when compared to conduction cooling techniques. In addition, it presents the advantage of allowing a single cryocooler serving a number of hot devices spread apart.

Experimental tests for pumping of liquid nitrogen showed that an ion-drag meso-pump is able to provide enough fluid flow to attain an acceptable heat transfer from chips. The mass flow rate was found from the application of an energy balance in the cryogenic cooler. Another effort of the research focused on the evaluation of different ion-drag micro-pumps designs based on the generated pressure head and power consumption. These tests were carried out with HFE-7100 cooling fluid at room temperature. The micro-pumps were fabricated on alumina or silicon wafers using photolithography techniques to pattern emitter and collector electrodes. A numerical simulation of the electric field resulted in a field onset that compares realistically with data available for dielectric fluids. The next steps of the research include the optimization of the micro-pumps by means of experimental and numerical simulations, and its implementation in a cryocooler loop for pumping of liquid nitrogen.

5. ACKNOWLEDGMENTS

Financial support of this project by the Advanced Thermal and Environmental Concepts Inc. (ATEC, Inc. College Park, MD) through a sub-contract for a project funded by the Office of Naval Research (ONR) is greatly appreciated. The authors also would like to thank NASA Goddard Flight Center for their technical support and assistance in conducting closed loop cryogenics pumping tests. Efforts of Jeff Didion and Mario Martins of NASA were particularly instrumental in the successful completion of the experiments.

6. REFERENCES

[1] Stuetzer, Omar M., 1959, "Ion Drag Pressure Generation," *Journal of Applied Physics*, Vol. 30, No. 7, p. 984-994

[2] Sharbaugh, H. A., Walker, G. W., 1985, "The Design and Evaluation of an Ion-drag Dielectric Pump to Enhance Cooling in a Small Oil-filled Transformer," *IEEE Transactions on Industry Applications*, Vol. 21, p. 950-5

[3] Barbini, G., Coletti, G., 1995, "Influence of Electrode Geometry on Ion-drag Pump Static Pressure," *IEEE Transactions on Dielectric and Electrical Insulation*, Vol. 2, No. 6, p. 1100-5

[4] Bryan, J.E and Seyed-Yagoobi, J., 1992, "An Experimental Investigation on Ion-drag Pump in a Vertical and Axisymmetric Configuration," *IEEE Transactions on Industry Applications*, Vol. 28, p. 310-16

[5] Bryan, J.E and Seyed-Yagoobi, J., 1994, "Analysis of 2-dimensional Flow Fields Generated by a 1-Electrode-pair Ion-drag Pump," *IEEE Transactions on Dielectric and Electrical Insulation*, Vol. 1, No. 3, p. 459-467

[6] Bryan, J.E and Seyed-Yagoobi, J., 1990, "Ion-drag Electrohydrodynamic Pumping Selecting an Optimum Working Fluid," *Tenth International Conference on Conduction and Breakdown in Dielectric Liquids* (Cat. No.90CH2812-6), p. 603, 316-22

[7] Bryan, J.E., 1990, "An Experimental Study of Ion-drag Pumping in a Vertical Axisymmetric Configuration," Master's Thesis, Texas A&M Univ, College Station, TX.

[8] Castaneda, J.A. and Seyed-Yagoobi, J., 1991, "Electrohydrodynamic Pumping of Refrigerant 11," *1991 IEEE Industry Applications Society Annual Meeting* (Cat. No.91CH3077-5), p. 2 vol. 1910, 500-3 Vol. 1.

[9] Ohadi, M.M., Darabi, J., and Roget, B., 2001, "Electrode Design, Fabrication, and Materials Science for EHD-Enhanced Heat and Mass Transport," Annual Review of Heat Transfer, Edited by C. L. Tien, Vol. 11, pp. 563-623, Begell House, Inc, New York.

[10] Rada, M., Darabi, J., Ohadi, M.M., Lawler, J., 2001, "Electrohydrodynamic Pumping of Liquid Nitrogen Using a Mesoscale Ion-Drag Pump," *Proceedings of IECEC 01 Energy Technologies Beyond Traditional Boundaries*, Savannah, Georgia.

[11] Gallagher, T. J., 1975, *Simple Dielectric Liquids: Mobility, Conduction, and Breakdown*, Oxford University Press, Ely House, London.

Copyright © 2002 by ASME

Downloaded From: https://proceedings.asmedigitalcollection.asme.org on 07/02/2019 Terms of Use: http://www.asme.org/about-asme/terms-of-use

Table 1 - Thermophysical properties of two working fluids tested.

Thermophysical Property	HFE-7100	Liquid Nitrogen
Boiling Point at 1 atm (^oC)	61	-196
Liquid density (kg/m^3)	1402	808
Liquid kinematic viscosity (cSt)	0.38	0.205
Liquid specific heat (J/kg-K)	1253	2030
Dielectric strength (kV/mm)	11	>10
Thermal conductivity (W/mK)	0.07	0.1411
Dielectric constant	7.40	1.45

Table 2 - Conduction thermal resistance in different test conditions.

Test No.	$\dot{Q}$ (W)	T_0 (K)	T_1 (K)	T_2 (K)	R (K/W)
1	1.37	83.33	82.97	80.87	2.06
2	1.37	83.23	82.86	80.62	2.18
3	1.37	84.64	84.37	80.86	2.95
4	2.14	93.30	88.60	91.84	2.88
5	2.14	83.47	82.69	79.51	2.21
6	3.08	86.56	84.08	81.23	2.53

Table 3 - Temperatures in the liquid nitrogen loop wall before and after the application of 3.16 W in the electric heater.

Measured temperatures	Before application of heat	After application of heat
T_{w0}	81.4	87.4
T_{w1}	81.4	87.4
T_{w2}	81.4	86.4

Downloaded From: https://proceedings.asmedigitalcollection.asme.org on 07/02/2019 Terms of Use: http://www.asme.org/about-asme/terms-of-use

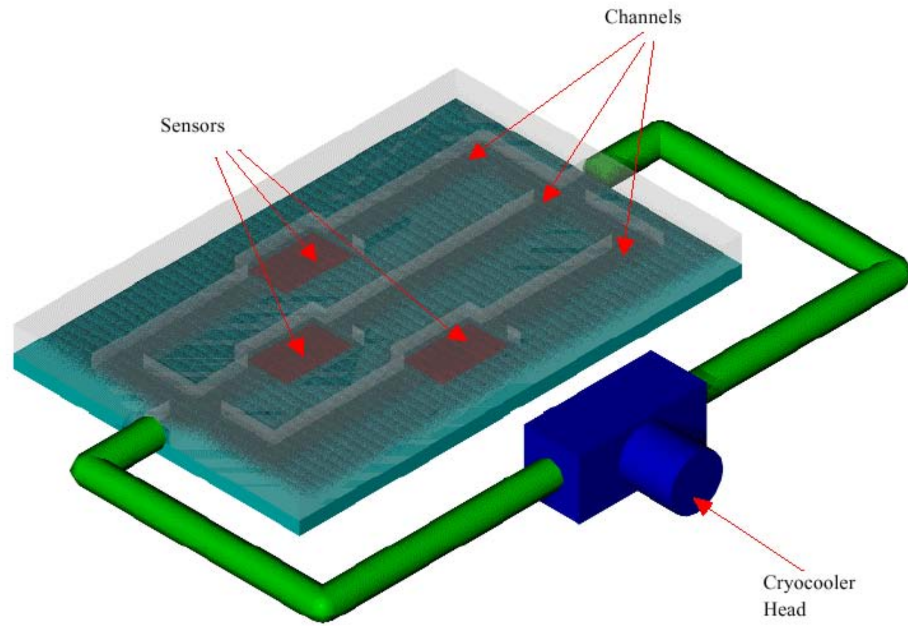

Fig. 1 Source integrated cooling of sensors at cryogenic temperatures

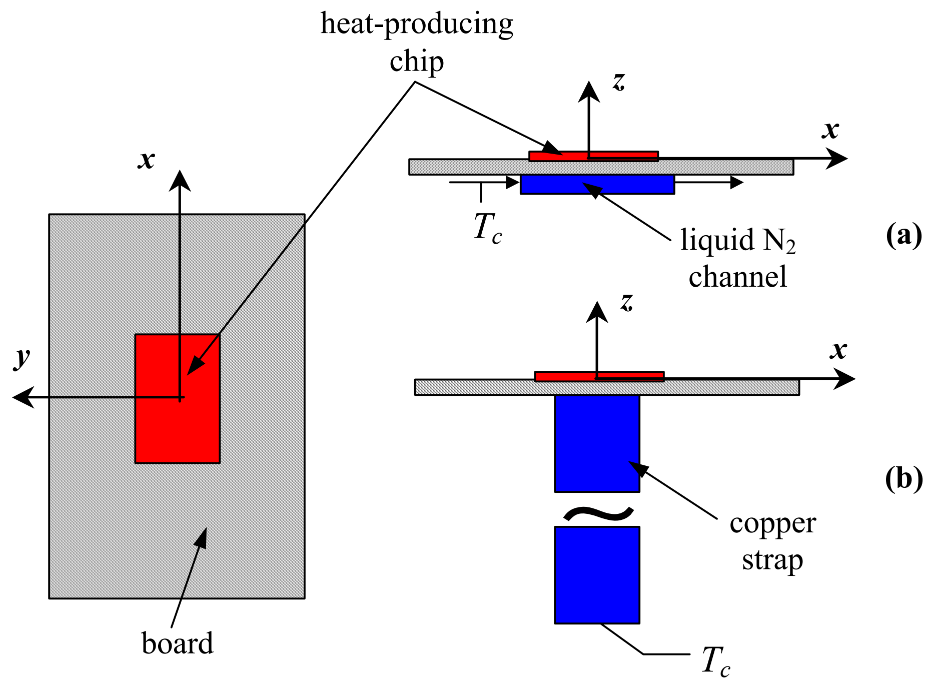

Fig. 2 Cooling of a high-power chip at a cryogenic temperature T_c: (a) employing the concept of liquid nitrogen cooling; (b) employing a copper strap directly attached to the cryocooler.

Downloaded From: https://proceedings.asmedigitalcollection.asme.org on 07/02/2019 Terms of Use: http://www.asme.org/about-asme/terms-of-use

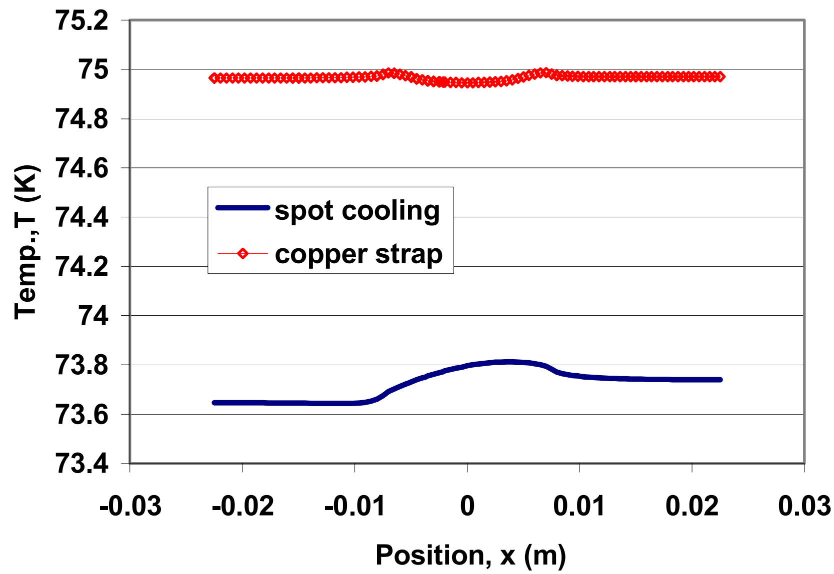

Fig. 3 Temperature distribution in the chip for case (a): spot cooling with liquid nitrogen; and (b): conduction through a copper strap.

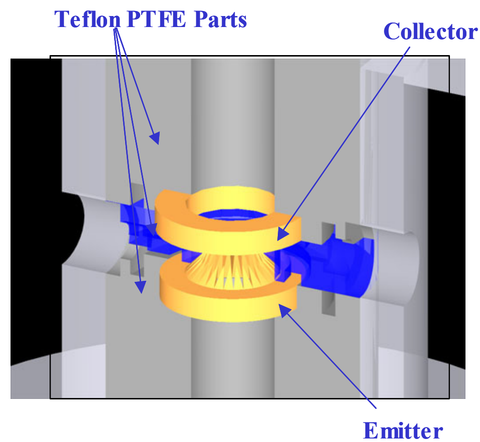

Fig. 4 EHD liquid nitrogen (LN_2) injection meso-pump with one stage.

Downloaded From: https://proceedings.asmedigitalcollection.asme.org on 07/02/2019 Terms of Use: http://www.asme.org/about-asme/terms-of-use

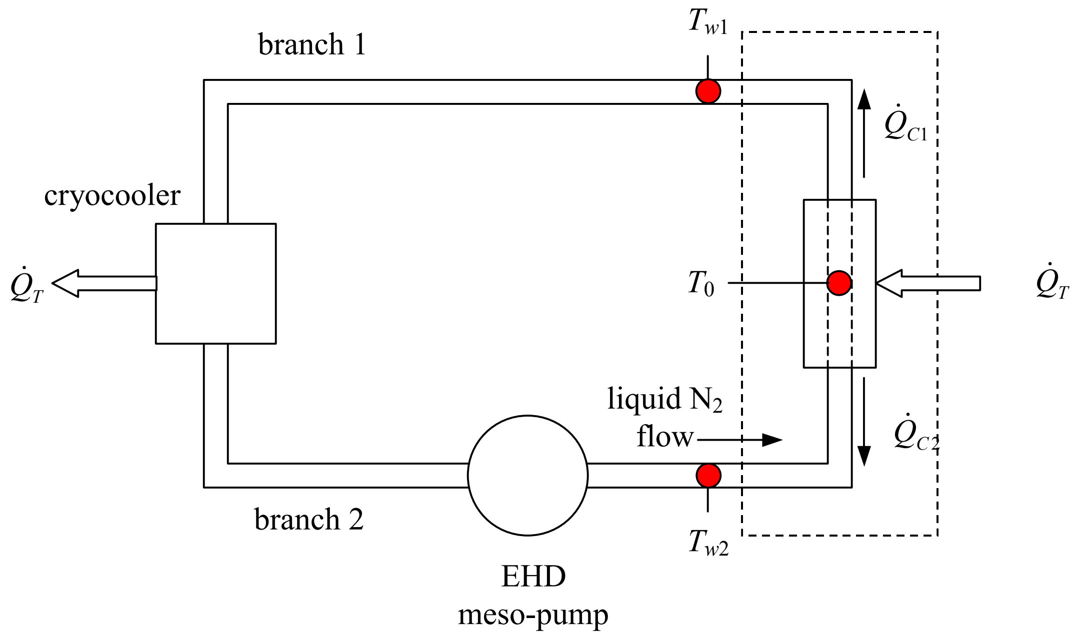

Fig. 5 Schematic of the liquid nitrogen EHD meso-pump loop

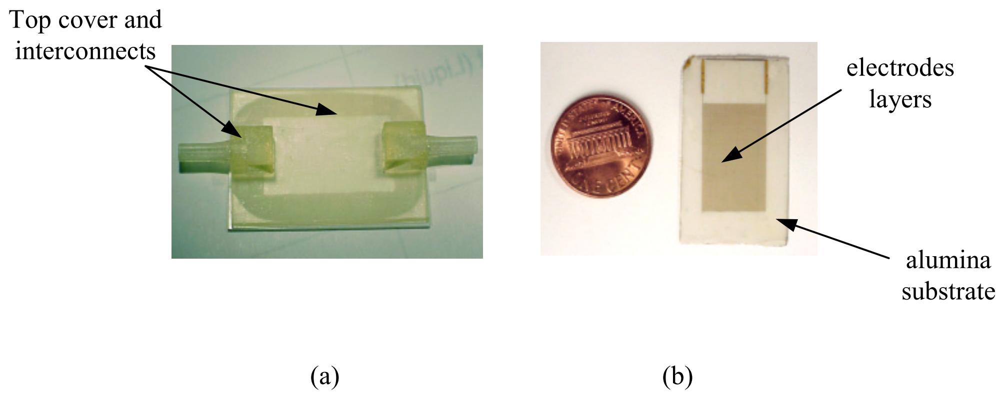

Fig. 6 Ion-drag micro-pump: (a) Assembled micro-pump; (b) micropump substrate (without top cover and interconnects).

Downloaded From: https://proceedings.asmedigitalcollection.asme.org on 07/02/2019 Terms of Use: http://www.asme.org/about-asme/terms-of-use

Fig. 7 Example of micro electrodes that have been fabricated in the micro fabrication at the University of Maryland at College Park: (a) saw-tooth emitter and plain collector separated by 25 µm; (b) plain emitter and collectors separated by 50 µm.

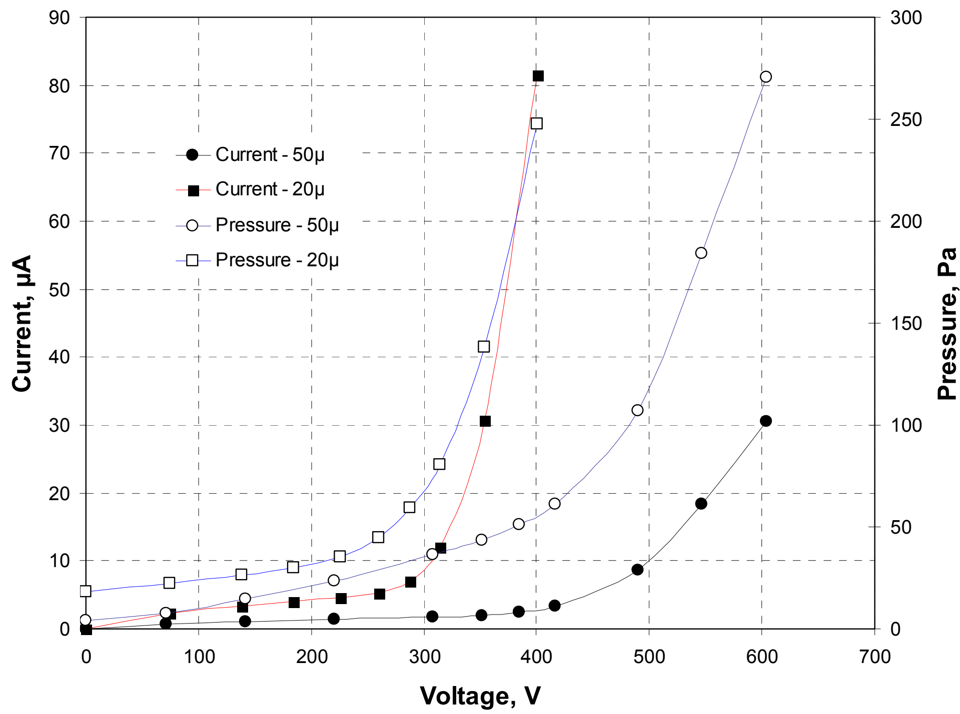

Fig. 8 Pressure head and electric current versus applied voltage for saw-tooth emitters and plain collectors. Electrode spacings of 20 and 50 µm.

Downloaded From: https://proceedings.asmedigitalcollection.asme.org on 07/02/2019 Terms of Use: http://www.asme.org/about-asme/terms-of-use

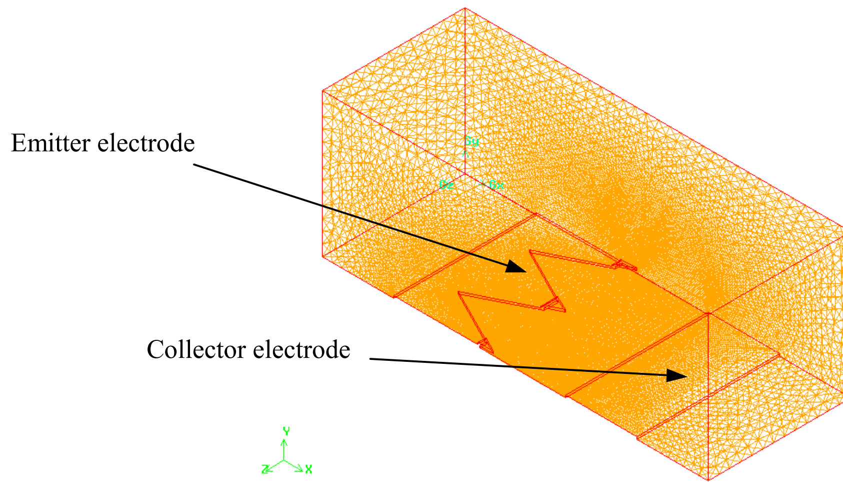

(a)

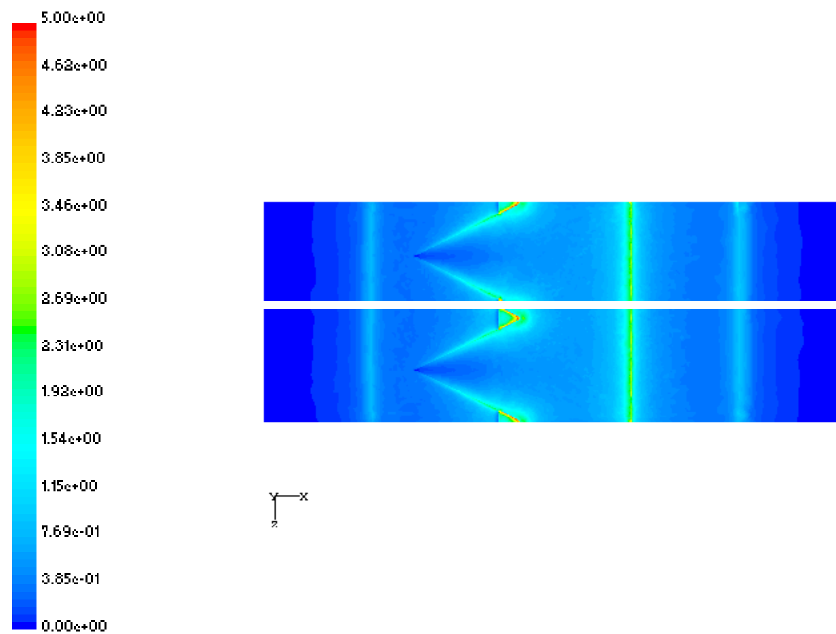

(b)

Fig. 9 Numerical simulation of the electric field between the emitter and collector: (a) grid mesh; (b) electric field distribution.

Downloaded From: https://proceedings.asmedigitalcollection.asme.org on 07/02/2019 Terms of Use: http://www.asme.org/about-asme/terms-of-use